



## Contents

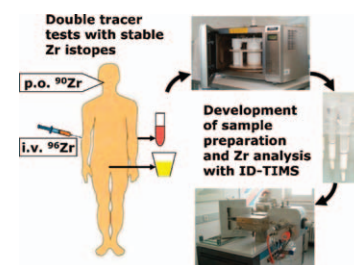
### Regular articles

1–8

#### Method development for thermal ionization mass spectrometry in the frame of a biokinetic tracer study with enriched stable isotopes of zirconium

Matthias B. Greiter, Vera Höllriegel, Uwe Oeh

► Development of ID-TIMS for all stable Zr isotopes in several compositions at once. ► Optimization for trace amounts of Zr in human blood plasma and urine. ► Ionization enhancement by carbon coated rhenium single filaments. ► Multiple channel electron multipliers as detectors. ► Tracer detection limits below 1 ng ml<sup>-1</sup>.

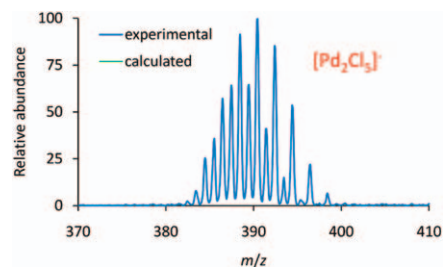


9–14

#### Clustering of palladium(II) chloride in acetonitrile solution investigated by electrospray mass spectrometry

Vojtěch Šádek, Detlef Schröder, Nikos G. Tsierkezos

► Sampling of solution properties via ESI-MS. ► Pronounced aggregation of PdCl<sub>2</sub> in acetonitrile solution. ► Partial reduction of anionic clusters to palladium(I). ► Implications for palladium catalysis.

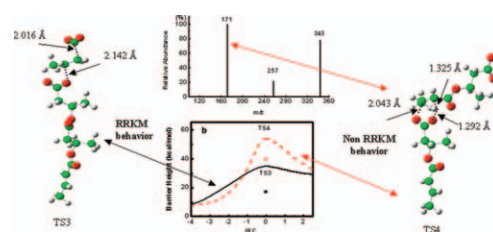


15–24

#### A combined theoretical and experimental study of mechanisms of fragmentation active for PHB oligomers in negative-ion mode multistage mass spectrometry

Henryk Bednarski, Karl Sohlberg, Marian Domański, Jan Weszka, Grażyna Adamus, Marek Kowalczyk, Vasile Cozan

► Identification of an alternative “direct” fragmentation channel of PHB. ► According to the RRKM theory this should be dominant fragmentation process. ► MS spectra consistent are with the dominance of indirect fragmentation processes. ► Thermal and CID MD simulations confirm the presence of the direct pathway.

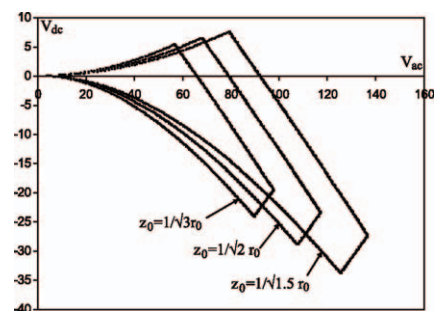


## 25–28

### Theoretical study of the effect of ion trap geometry on the dynamic behavior of ions in a Paul trap

I. Ziaeeian, S.M. Sadat Kiai, M. Ellahi, S. Sheibani, A. Safarian, S. Farhangi

► We worked on the stretched Paul trap with changing the size of  $n$  in  $z_0 = (1/\sqrt{n})r_0$  parameter. ► With decreasing  $n$ , the ion trajectory is more restricted in the  $r$  and  $z$  directions. ► With decreasing  $n$ , the first stability region in  $a-q$  plane is compacted. ► With decreasing  $n$ , the first stability diagram in  $U-V$  plane for a typical ion is enlarged. ► With decreasing  $n$ , the fractional mass resolution is higher.

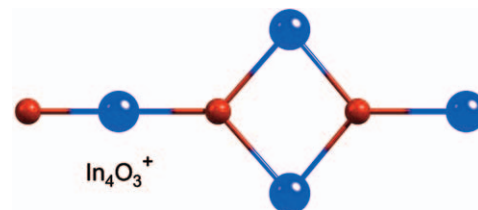


## 29–35

### Photodissociation of indium oxide cluster cations

A.M. Knight, B. Bandyopadhyay, C.L. Anfuso, K.S. Molek, M.A. Duncan

► Indium oxide cluster cations are produced in a laser vaporization source and analyzed with time-of-flight mass spectrometry. ► Cluster ions are mass-selected and photodissociated at 355 nm. Prominent photofragments are  $\text{In}^+$ ,  $\text{In}_2\text{O}^+$ ,  $\text{In}_2\text{O}_2^+$ ,  $\text{In}_3\text{O}^+$  and  $\text{In}_3\text{O}_2^+$ . ► Density functional theory finds linear structures for many small clusters and confirms the relative stabilities of prominent photofragments.

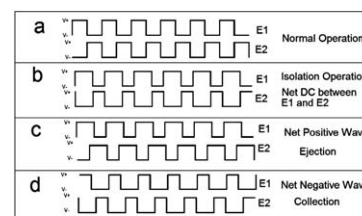


## 36–40

### Simulation of duty cycle-based trapping and ejection of massive ions using linear digital quadrupoles: The enabling technology for high resolution time-of-flight mass spectrometry in the ultra high mass range

Jeonghoon Lee, Maxwell A. Marino, Hideya Koizumi, Peter T.A. Reilly

► The duty cycle of the waveforms applied to a digital ion guide can be used to trap and eject ions. ► Adding Linac electrodes to the guide permits ion to be trapped and collected in front of the exit end cap electrode. ► Collected ions can be ejected in plug with well-collimated trajectories into the acceleration region of an oa-TOFMS. ► Trapping, collecting and ejection by this method permits ions of ANY mass-to-charge ratio to be injected into a oa-TOFMS in collimated trajectories with controlled kinetic energy distributions. ► This technology will enable high resolution TOFMS in the ultra high mass range ( $m/z > 20$  kDa).



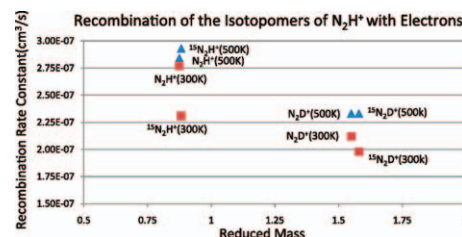
Changing the Duty Cycle of Digital Ion Guide Waveforms

## 41–44

### Effect of isotopic content on the rate constants for the dissociative electron-ion recombination of $\text{N}_2\text{H}^+$

Patrick A. Lawson, David Osborne Jr., Nigel G. Adams

► The heavier isotopomers of  $\text{N}_2\text{H}^+$  recombined slower with electrons. ► This data is compatible with  $\text{N}_2\text{D}^+/\text{N}_2\text{H}^+$  ratios found in the interstellar medium. ►  $^{15}\text{N}$  had lessened, but similar effects on recombination compared to D substitution. ► Isotopic effects on dissociative recombination were compared.

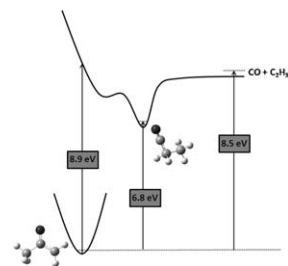


## 45–50

**Dissociative photoionization of  $\text{CH}_3\text{C}(\text{O})\text{CH}_2$  to  $\text{C}_2\text{H}_5^+$** 

Bridget W. Alligood, Caroline C. Womack, Matthew D. Brynteson, Laurie J. Butler

► 10.5 eV ionization of  $\text{CH}_3\text{C}(\text{O})\text{CH}_2$  yields  $\text{C}_2\text{H}_5^+$  fragments rather than parent ions. ► Our results characterize the efficient dissociative ionization of  $\text{CH}_3\text{C}(\text{O})\text{CH}_2$  to  $m/z = 29$ . ► A minor dissociation channel of  $\text{CH}_3\text{C}(\text{O})\text{CH}_2$  is confirmed, that to  $\text{C}_2\text{H}_5 + \text{CO}$ . ► For this system, there are 2 sources of  $m/z = 29$ , not just the ionization of  $\text{C}_2\text{H}_5$ . ► Care should be taken in assigning  $m/z = 29$  signal in multicomponent systems.

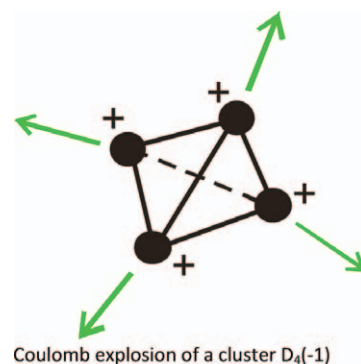


## 51–56

**High-charge Coulomb explosions of clusters in ultra-dense deuterium  $\text{D}(-1)$** 

Leif Holmlid

► Laser ionization of small clusters  $\text{D}_3$  and  $\text{D}_4$  of ultra-dense deuterium give maximum-charge Coulomb explosions. ► The kinetic energy release (KER) in a  $\text{D}_4$  cluster gives 945 eV to each  $\text{D}^+$  ion. ► By cooling the clusters on a solid surface, it is possible to decrease the rotational energy of the clusters, which gives a shorter bond distance. ► The rotational energy of a small cluster of ultra-dense deuterium is large even at small  $J$  numbers due to the bond distance of 2.3 pm.



## 57–65

**Ionic and vibrational properties of an ultra-low ionization potential molecule: Tetrakis(dimethylamino)ethylene**

Nasrin Mirsaleh-Kohan, Wesley D. Robertson, Jason Lambert, R.N. Compton, Serge A. Krasnokutski, Dong-Sheng Yang

► We measure refined adiabatic potential of jet-cooled TDAE. ► Upper bounds of the adiabatic ionization potential measured from the electron ionization and laser ionization are  $5.3 \pm 0.2$  and  $5.20 \pm 0.05$  eV, respectively. ► The adiabatic ionization potential of TDAE is about 0.6 eV lower than its vertical ionization potential. ► TDAE has a non-planar structure and its changes upon ionization.

